Article

Constant Pressure CO2 Replacement of CH4 in Different Hydrate Environments: Structure and Morphology

Andrea Rossi, Michele Ciulla, Valentino Canale, Marco Zannotti, Marco Minicucci, Pietro Di Profio,* and Rita Giovannetti*

Read Online

ACCESS | 📊 Metrics & More | 📖 Article Recommendations | 🆂 Supporting Information

ABSTRACT: Gas hydrates (GHs) are solid, ice-like compounds composed of water molecules forming a lattice structure that hosts gas molecules, produced under high pressure and low temperature. The structure of the hydrate structure is affected by the surrounding environment, and in this context, a structural characterization of GHs prepared in different environments, ultrapure (UP) water, seawater, synthetic sand, natural sand, and sodium dodecyl sulfate, has been proposed. In particular, the Raman spectroscopy has been used to investigate the structural changes in the water cages, the gas uptake in the hydrate structure, the CH_4 cage occupancies, the hydration number, and the yield of carbon dioxide replacement at constant pressure. For this comparison, CH_4-hydrates, CO_2-hydrates, and CH_4/CO_2-hydrates (obtained from an implemented replacement process) were prepared in five different experimental conditions mentioned above and structurally characterized. From Raman investigation, pure CH_4-hydrates displayed almost full (>95%) occupation in the large cage and a significant change in the small cage occupation related to the different tested media. The cage occupancy calculation of CO_2/CH_4-hydrates showed that a higher yield of replacement can be obtained in UP water and that CH_4-hydrates in natural sand and in seawater, which are the most representing of natural environments, displayed a good replacement of CH_4 with CO_2. Additionally, the *ex situ* morphological characterization of the GHs by scanning electron microscopy (SEM) allowed the highlighting of morphological differences among the investigated samples.
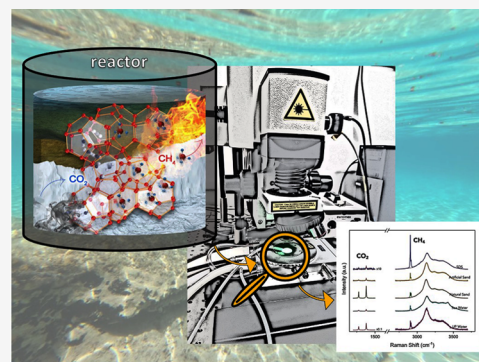
1. INTRODUCTION

Gas hydrates are nonstoichiometric compounds formed when water and gas molecules are contacted under high pressures and low temperatures. In these conditions, the water molecules arrange into H-bonded structures, which can host gas molecules interacting with the cages through dispersive forces.[1] Clathrate hydrates have three main crystallographic structures: structure I (sI), structure II (sII), and structure H (sH). Structure sI, composed of a small pentagonal dodecahedral cage (5^{12}) and a large tetrakaidekahedral cage with 12 pentagonal and 2 hexagonal faces ($5^{12}6^2$), can host only small gas molecules (0.40−0.55 nm), such as methane, ethane, carbon dioxide, hydrogen sulfide, etc. Structure sII, also containing the small 5^{12} cages in addition to a large hexacaidekahedral cage with 12 pentagonal and 4 hexagonal faces ($5^{12}6^4$), can host molecules ranging from 0.6 to 0.7 nm, such as propane and iso-butane. Structure sH, composed of the small 5^{12} cages, intermediate $4^35^66^3$ cages (with 3 square, 6 pentagonal, and 3 hexagonal faces), and large icosahedral cages, $5^{12}6^8$ (containing 12 pentagonal and 8 hexagonal faces), hosts both small and large molecules (size range 0.8−0.9 nm) like methane + neohexene and methane + cycloheptane.[2] Natural gas hydrates (NGHs) are considered a potential energy source since it has been estimated that a huge amount of natural gas is stored in the form of

hydrates.[3] The most promising technique that can be used to exploit this energy source is the exchange process, which consists of the injection of CO_2 in the CH_4-reservoirs, exploiting the fact that CO_2 forms relatively more stable hydrates than methane.[4] On the other hand, the exchange process is not complete because the CO_2 can preferentially occupy the large cages; therefore, it is necessary to couple the exchange process with other techniques, such as depressurization to maximize the yield.[5,6]

Raman spectroscopy is a powerful tool to characterize the GH structures and monitor the replacement process since it is a nondestructive technique, easily applicable, and in some cases portable.[7] The Raman signal of CH_4 in the gas and liquid phases is located at 2917 and 2911 cm^{-1}, respectively; however, when the CH_4 is hosted in the hydrate cages, the signal undergoes splitting as predicted by the loose-cage tight-cage theory, which is related to the type of cages and therefore can be used to

identify the structure type.[8] In the sI hydrate, the CH_4 signal splits into two bands at ~2905 and ~2915 cm^{-1} for large and small cages, respectively, with a theoretical intensity ratio of 3:1. For sII hydrate, the intensity of the two signals is reversed with respect to sI hydrates with an intensity ratio of 1:3. The CH_4 signal in the sH structure does not split the signal into two bands and is characterized by a broader band at 2913 cm^{-1}.[9] The CO_2 replacement process can be monitored by the resulting appearance of the characteristic Fermi dyad of CO_2 at ~1275 cm^{-1} (v1) and ~1380 cm^{-1} (v2)[10] and by a decrease of the intensity of the signal related to methane in the large cages since CO_2 can preferentially occupy the large cages in the sI structure.[11]

In this work, single CO_2 and CH_4 hydrates and mixed CO_2/CH_4-hydrates were obtained by a constant pressure replacement process in UP water, seawater, natural sand, synthetic sand, and SDS solution using a custom-made reactor. Successively, the hydrates were *ex situ* structurally and morphologically characterized by Raman spectroscopy and scanning electron microscopy (SEM), respectively. SEM images were acquired to investigate the morphological differences between the samples prepared in different conditions, while Raman spectroscopy was used for the qualitative characterization of all of the specimens by identifying the chemical fingerprints of CO_2 and CH_4 molecules in the gas hydrate cages. Additionally, the application of the van der Waals and Platteeuw (vdWP) thermodynamic models[12] allowed us to obtain the CH_4 cage occupancy of pure CH_4-hydrates and CO_2/CH_4-hydrates obtained after the replacement process. Previous studies have addressed the issue of the CH_4/CO_2 exchange by focusing on a limited set of experimental exchange media and investigation techniques, and they were mainly carried out under pressure dropping conditions, which is clearly different from the constant pressure to be expected in a natural gas hydrate field.[10,13] The present study is an advancement in the knowledge of CH_4/CO_2 exchange in simulated natural media, as it describes the kinetics of the process and structural features of the obtained hydrates under constant pressure conditions, which are closer to the real-case scenario.

2. EXPERIMENTAL SECTION

2.1. Materials. CH_4 and CO_2 were provided by SOL S.p.A. CH_4 was 2.5 grade (99.5% methane), and CO_2 was SS-grade (99.8% carbon dioxide). CH_4/CO_2 mixtures were prepared by measuring the respective amounts with a mass flow meter (F131 M series, Bronkhorst, The Netherlands). SDS (sodium dodecyl sulfate, >95.0%, gas chromatography grade) was provided by Sigma-Aldrich (Italy). It is a white powdery solid and is a well-known surfactant and hydrate promoter. Here, it was used in ultrapure water (UPw) solution, as reported in Table 1. The UPw used for the hydrate preparation was produced by a Milli-Q water purification system (Millipore Merck). Seawater for this experiment was sampled offshore in the Adriatic Sea,

Table 1. Media Used for the Synthesis of CO_2, CH_4, and CO_2/CH_4-Hydrates and Their Respective Concentrations and Volumes

	CH$_4$-hydrate	CO$_2$-hydrate	CO$_2$/CH$_4$-hydrate
UP water	1 mL	1 mL	1 mL
seawater	1 mL	1 mL	1 mL
SDS	0.2 mg/mL		0.2 mg/mL
natural sediment	1.396 g/mL	1.336 g/mL	1.363 g/mL
synthetic sediment	1.335 g/mL	1.321 g/mL	1.364 g/mL

with the chemical−physical composition reported in Table S2, and used without further purification. The two different types of sediments used in this study were characterized to obtain the grain size and chemical composition (Figure S9 and Table S3); these were, namely, synthetic sand and natural sand, and they have been used in combination with ultrapure water as reported in Table 1.

2.2. Apparatus. A detailed illustration of the reactor used to produce GHs is reported in Figure 1. The reactor has been designed and assembled by RDPower s.r.l. (Terni, Italy), and it allows the preparation of gas mixtures of any desired composition. The reactor is composed of AISI 316L stainless steel with an internal volume of 350 mL and an operating pressure that can reach up to 20 MPa. Operating temperatures were controlled by a cooling/heating Peltier unit, which allows temperature control in the range of 253−353 K. The gas flow inside the reactor was regulated by a CC Series micro metering valve provided by Tescom while being measured by an F131 M series thermal mass flow meter provided by Bronkhorst (Bronkhorst High-Tech B.V., Netherlands) with a measuring range of 50−2000 N mL/min and an operating pressure of 40 MPa. The reactor is equipped with a 4−20 mA pressure transducer purchased by Gems Sensors & Controls (United Kingdom) with a measuring range of 0−40 MPa and three resistive temperature detectors (RTD) PT100 class 1/3 DIN purchased by OMEGA Engineering, Inc. Two further pressure transducers are assembled along the gas loading line before and after the metering valve to measure the pressure during the mixture preparation process. An Arduino microcontroller was used to process the temperatures of the reactor and drive the Peltier power. The temperature set point is kept constant by using a PID algorithm embedded into the Arduino controller. The gas mixture composition was monitored by IR detectors (Premier series of IR gas sensors by Dynament (UK) for CO_2 and CH_4). The apparatus for gas quantification was previously standardized by using gaseous mixtures with known ratios of CO_2 and CH_4. A more detailed explanation of the reactor can be found elsewhere.[14−16]

2.3. Synthesis of Gas Hydrates. Hydrate samples were synthesized in a customized copper sample holder (Figure 2), which can be directly transferred into a Linkam THMS600 cell that allows Raman characterization at low temperatures. CO_2-hydrates were prepared by filling the cylindrical copper wells with the additives necessary for the formation of hydrates in different media, as described in Table 1, and placed inside the reactor. The temperature was then decreased by using a temperature ramp (1 °C/min) at a constant pressure of 3.5 MPa until reaching a set point temperature of 1 °C. The pressure of 3.5 MPa was selected due to the liquefaction of CO_2 at higher pressures; the reactor was kept under these conditions for 24 h. Successively, the formed hydrates were stabilized by the application of a subcooling (−25 °C), and the pressure was gradually released to allow the opening of the reactor and removal of the formed hydrate.

The CH_4-hydrates were prepared by following the same operating process as the CO_2 hydrates and the same media described in Table 1, except for the operating pressure, which was set at 7 MPa. The CO_2 exchange experiments were performed on newly produced CH_4-hydrates by using the same conditions previously described and the same media summarized in Table 1. Specifically, after the formation of CH_4-hydrates and their stabilization for 5 days, the pressure was decreased from 7 to about 3.5 MPa, and the cooled CO_2 was allowed to flux into the reactor at constant pressure (Figures S7 and S8). During the gas-phase swapping, the hydrate was stabilized by decreasing the temperature to avoid the dissociation of CH_4-hydrates. The IR detector was connected at the outlet line to monitor the percentage of CO_2 and the residual level of CH_4 in the reactor. When the detector displayed 100% of CO_2 inside the vessel, the system was isolated and the CH_4-hydrate under a CO_2 atmosphere was kept at 1 °C for a further 5 days.

2.4. Raman Measurements. Raman spectra were obtained with a micro-Raman setup (Figure 2) that consists of a Czerny−Turner spectrometer (iHR320 Horiba Scientific) equipped with three different gratings 600, 1800, and 2400 g/mm that allow reaching a maximum resolution of 0.007 nm and an open space microscope to accommodate a Linkam THMS600 cell for low/high-temperature conditions (ranging from −195 to 600 °C). The samples, prepared in a customized copper sample holder, were transferred from the liquid nitrogen to the Linkam
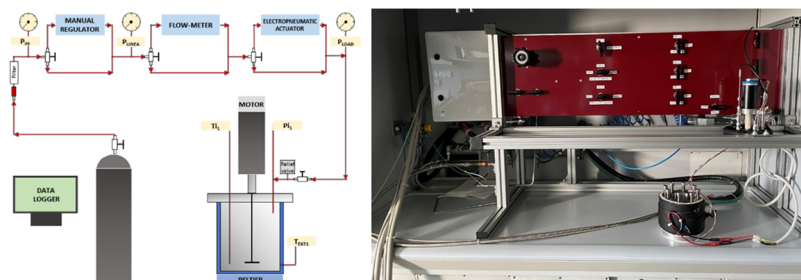
Figure 1. Scheme of the multiple-reactor apparatus (left); picture of the reactor (right panel). Adapted with permission.[15] Copyright 2017. American Chemical Society.
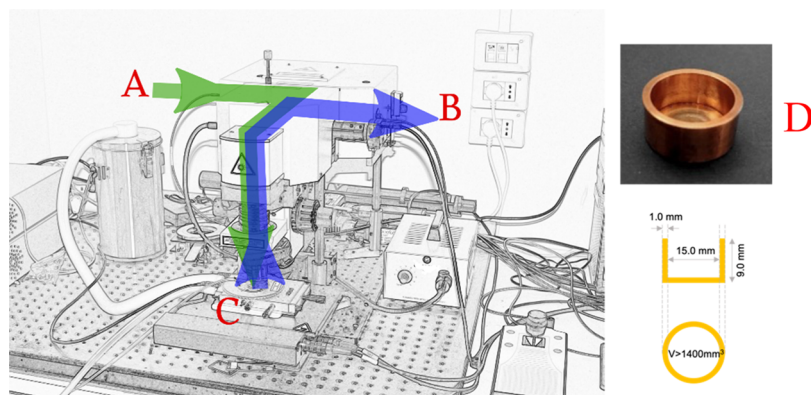

Figure 2. Raman setup: green arrow: incident laser beam path; blue arrow: backscattered laser beam path; (A) microscope laser beam input to the sample; (B) microscope laser beam output to the spectrometer; (C) low-temperature device; and (D) customized copper sample holder.

sample holder. Once the operating temperature had been reached, the chamber was flushed with nitrogen to eliminate the condensed water that formed due to the low operating temperature.

Raman spectra of CO_2 hydrates were obtained with grating 600, a 10 s acquisition time, and 30 accumulations, green laser (532 nm), temperature 213.15 K, in the range from 900 to 4200 cm^{-1}. Signals were fitted by the Voigt function. Raman spectra of methane hydrate samples were acquired with a 10 s acquisition time, 30 accumulations, grating 2400, and green laser (532 nm) at 173.15 K in the range from 2600 to 2700 cm^{-1}. CH_4 signals were deconvoluted by the Voigt function for CH_4-hydrates and CH_4/CO_2-hydrates, respectively (Figures S10 and S11). Raman spectra of CH_4/CO_2-hydrate, following replacement processes, were obtained with a 10 s acquisition time, 30 accumulations, grating 2400, and green laser (532 nm) at 173.15 K in the ranges 1000−1600 and 2800−3800 cm^{-1}.

2.5. SEM Measurements. The morphological characterization of hydrates was performed by field-emission SEM, Sigma 300, Zeiss, coupled with an energy-dispersive X-ray spectrometer (EDX, Quantax, EDS, Bruker) and with temperature-controlled equipment (Coolstage by Seben). The samples were stored in liquid nitrogen and transferred to the cooling stage in the SEM instrument at a temperature of −25 °C. In this case, a representative portion of the hydrate samples was transferred to the homemade SEM sample holder and transferred to the cool stage (the selection and cutting operation of the representative portion of the sample were carried out in liquid nitrogen).

3. RESULTS AND DISCUSSION

The pressure and temperature profiles for the formation of methane, carbon dioxide, and CH_4/CO_2 mixed hydrates are reported in the Supporting Information (Figures S5 and S6). As described in the Experimental Section, in all cases, the experimental conditions are characterized by a high driving force giving rise to very stable hydrates, which do not change their state in time. Specifically, the P/T conditions were chosen in order to have an overpressure of 4.1 MPa for CH_4 and 2.1

MPa for CO_2, which values are strongly conducive to massive and stable hydrates.

The CH_4-, CO_2-, and exchanged CH_4-hydrates, prepared under different media, as previously described, were characterized by Raman spectroscopy, with the aim to highlight differences in the hydrate cages. The Raman spectrum of water is characterized by an intense signal in the region of 3000−4000 cm^{-1} related to the OH stretching bands (OHs).[17] This signal is related to the structure of water, and its shape changes according to the physical state of water as well as any interaction between water molecules and other substances by perturbing the stretching modes.[18] The Raman spectra of water can be divided into two regions associated with the symmetric and asymmetric OH bands of water.[19] Therefore, it is possible to follow the changes in the water structure by the relative evolution of these two partitions of the OH stretching region, as the evolution of the order and disorder of the water structure can be reflected from the values of their intensities. Thus, a spectral marker (S_D)[20] can be defined as the ratio of the asymmetric and the symmetric parts of the OH band and can be used to detect the strength of interaction among water molecules in the cages. The S_D index calculated for each specimen, based on the OH spectral deconvolution, highlights the symmetric against the antisymmetric contribution of the OH signals. Specifically, the center of the O−H stretching bond is located around 3325 cm^{-1}, corresponding to the isosbestic point, which divided the O−H stretching into two regions corresponding to symmetric and asymmetric stretching vibrations. It can be considered that the lower-frequency part of the spectrum (between 2900 and 3325 cm^{-1}) corresponds to the ordered solid phase, as this contribution is related to fully H-bonded atoms, whereas partly H-bonded and free O−Hs are expressed in the upper-frequency part, characteristic of the liquid phase.[19] The areas of the two
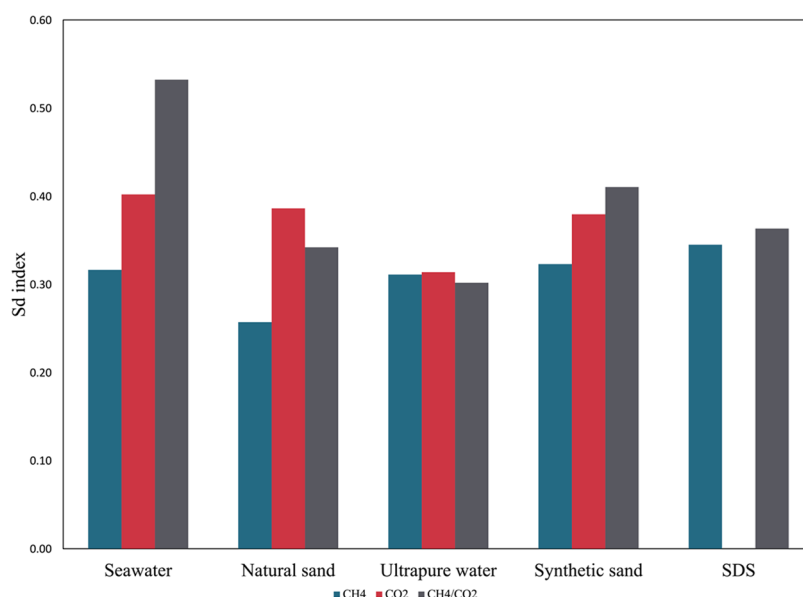
Figure 3. Comparison of the calculated S_D index between CH_4-hydrate, CO_2-hydrate, and CH_4/CO_2-hydrate.

regions were therefore measured in the range of 2800−3800 cm^{-1} for each Raman spectrum, and the ratios of the corresponding integrated intensities of the two regions (B/A), which represent the S_D concentration index,[21,22] were calculated and compared with each other (Figure 3). For the calculation of the S_D values, the Raman spectra of CH_4-hydrate (Figure S1), CO_2-hydrate (Figure S2), and CH_4/CO_2-hydrate (Figure S3) were deconvoluted by using a Voigt function, while the signal of methane was excluded from the calculation (Table S1). Before commenting on the results, it should be noted that generally hydrates have a certain amount of residual water, which depends on the driving force and the presence of promoters. In our case, the very high driving force adopted for hydrate formation (overpressure of 4.1 MPa for CH_4 and 2.1 MPa for CO_2; see the Experimental Section) reasonably led to a limited amount of residual water in all of the samples. In fact, Raman spectra show no clear evidence of the presence of free water.

The comparison of the S_D index shows no substantial difference in the symmetric/asymmetric stretching of OHs between CO_2-, CH_4-, and CO_2/CH_4-hydrates when they are prepared in UP water and in the presence of SDS (Figure 3). Incidentally, those two systems are the least and the most promoted, respectively, meaning that the former should have a higher amount of nonconverted water than the latter. However, as is apparent from Figure 3, their S_D ratios are almost the same, suggesting that the amount of free water is negligible in both systems. When hydrates are prepared in both seawater and synthetic sand, the S_D index reveals that CH_4-hydrate exhibits the highest rigidity (indicated by the lowest S_D), while CH_4/CO_2-hydrate shows the least rigidity (indicated by the highest S_D). This is because when water molecules are arranged in an orderly fashion, they can form a greater number of hydrogen bonds, resulting in a structure that is considered more rigid.

The hydrates prepared in natural sand show a trend similar to that observed for samples prepared in seawater and synthetic sand except for the S_D index calculated for CO_2-hydrate. Raman spectroscopy was also used to investigate the gas uptake in the hydrate cages in all of the prepared samples. The Raman characterization of CH_4-hydrates prepared in different media, namely, CH_4-hydrate in UP water, seawater, natural sand,

synthetic sand, and SDS, showed the presence of the characteristic signal of methane in the small and large cages (Figure 4).
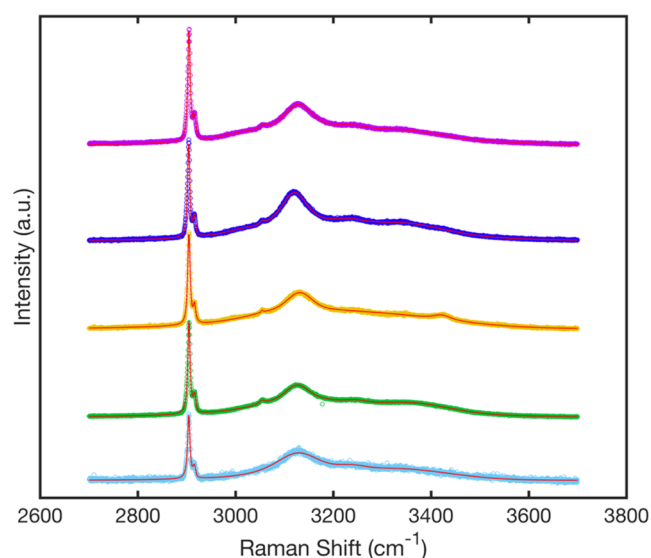

Figure 4. Raw Raman spectrum of CH_4-hydrates in natural sand (purple line), seawater (yellow line), UP water (cyan line), SDS (blue line), and artificial sand (green line) acquired with green (532 nm laser), 10 s, and 30 accumulations. The dotted red line shows the results of the fit.

The Raman spectra of CH_4-hydrates are characterized by two signals around 2905 and 2915 cm^{-1} assigned to methane in large and small cages, respectively. The peak intensities of methane could be used to determine the cage occupancy and hydration number by using the vdWP theory (see the SI for details).[12] The results of this calculation, applied to our specimens, identified the highest and lowest occupancy ratios in the CH_4-hydrates prepared in UP water and seawater, respectively. In all of the specimens, the degree of occupation in large cages is close to one, while the degree of methane occupation in small cages undergoes significant changes (Figure S4).

Raman spectra of CO_2-hydrates of all of the investigated specimens are reported in Figure 5 where it is possible to observe the characteristic peaks of CO_2, confirming the successful formation of CO_2-hydrate formation.
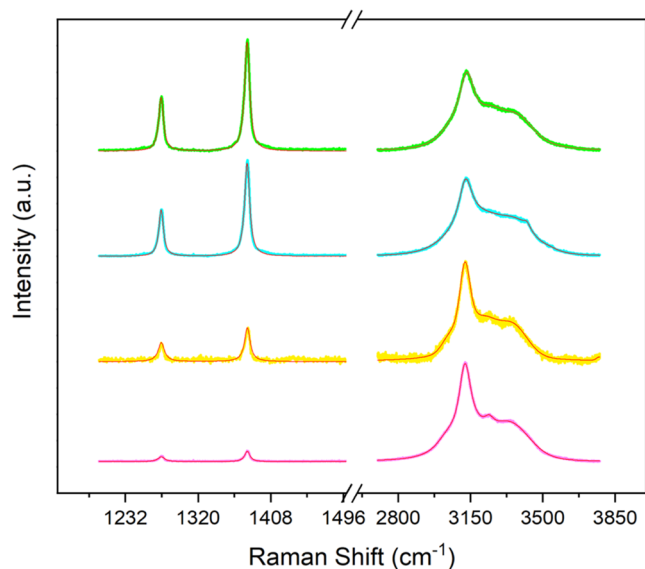

Figure 5. Raw Raman spectra of CO_2-hydrate in UP water (light purple line), seawater (cyan line), natural sand (green line), and artificial sand (yellow line), fitted curve (red line).

Unlike CH_4-hydrates, in this case, the two bands are not related to CO_2 in small and large cages; indeed, they appear because of a resonance effect, proposed by Fermi in 1931 that is related to the doublet structure in the region of the CO_2 symmetric stretching vibration, while the small peak at 1370 cm^{-1} is related to $^{13}CO_2$.[23] The Fermi resonance can be explained as a mixing of the upper state of a fundamental and the upper state of an overtone or combination band; after mixing, both states become partly fundamental and partly overtone or a combination of the two.

As a result of the mixing, the intensity of the fundamental is shared between the two bands involved, and the energies of the upper states move further apart, and so do the frequencies of the bands. Specifically, the two signals of CO_2 are related to the *v1* mode in Fermi resonance with the *2v1* mode (which is an overtone of the bending mode at 667 cm^{-1} that is not Raman active). Consequently, it is difficult to distinguish whether CO_2 occupies small or large cages only with the use of Raman spectroscopy, and there are contradictory opinions in the literature. In fact, some authors report the frequencies of stretching and bending vibrations of CO_2 in both SCs and LCs by deconvoluting the CO_2 signals.[24,25] However, this was criticized by other authors because they did not observe the splitting, predicted by the LCTC model, of the CO_2 bands in Raman spectra of sI CO_2 hydrate.[9,26,27] However, the aim of this work is to compare the uptake of CO_2 in the hydrate and not to carry out a quantitative analysis of CO_2; therefore, by considering that CO_2 can preferentially occupy large cages, and all of the samples were analyzed under the same conditions, the CO_2 signals were deconvoluted by a Voigt function and the fitted areas of the two signals were summed, related to the surface of OH signals and compared between the samples. It is important to emphasize that the spectra have been normalized

by applying the same factor used for the normalization of the OH signal at the isosbestic point.

Another interesting consideration about the CO_2 signals can be made by considering that the Fermi dyad split (Δ) increases with increasing density (ρ) due to the fact that the frequency shift of the lower band has greater density dependence than does the upper band. Therefore, it is possible to consider that all of the investigated samples possessed the same CO_2 density since no significant Raman shifts were observed on both CO_2-related signals, as expected (Table 2).

Table 2. Raman Shifts of *v1* and *2v2* of the CO_2 Fermi Dyad and the CO_2/H_2O Area of the Investigated CO_2-Hydrates

specimens	raman shift CO_2 *v1*	raman shift CO_2 *2v2*	CO_2/H_2O area
UP water	1275.5	1379.6	0.01
seawater	1275.3	1379.5	0.06
synthetic sand	1275.5	1379.7	0.02
natural sand	1275.2	1379.4	0.07

The raw Raman spectra of CO_2/CH_4-hydrates, obtained by replacement processes, prepared under the same conditions as the CH_4-hydrates previously discussed, highlighted the presence of both CO_2 and CH_4 in the hydrate structure, confirming the successful swapping between CH_4 and CO_2 (Figure 6). In this
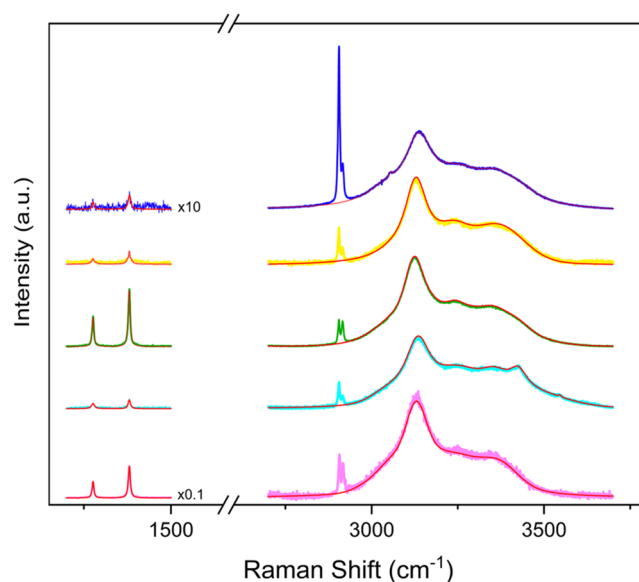

Figure 6. Raman spectra of CO_2/CH_4-hydrate obtained by a replacement process in artificial sand (yellow line), SDS (blue line), seawater (cyan line), natural sand (green line), and UP water (purple line).

case, the swapping method to produce the mixed hydrates allowed us to reduce chemical and physical disturbances within the system during the exchange process. This isobaric method preserves the starting methane hydrate structure, thus minimizing any negative effects on its stability. In particular, the constant pressure avoided the initial subcooling phase after the CH_4-hydrate formation and the sudden decrease in pressure inside the vessel, which could occur in the emptying and refilling method with CO_2. Moreover, maintaining a constant pressure can also help stabilize the temperature inside the reactor. This is another important aspect of the process since temperature
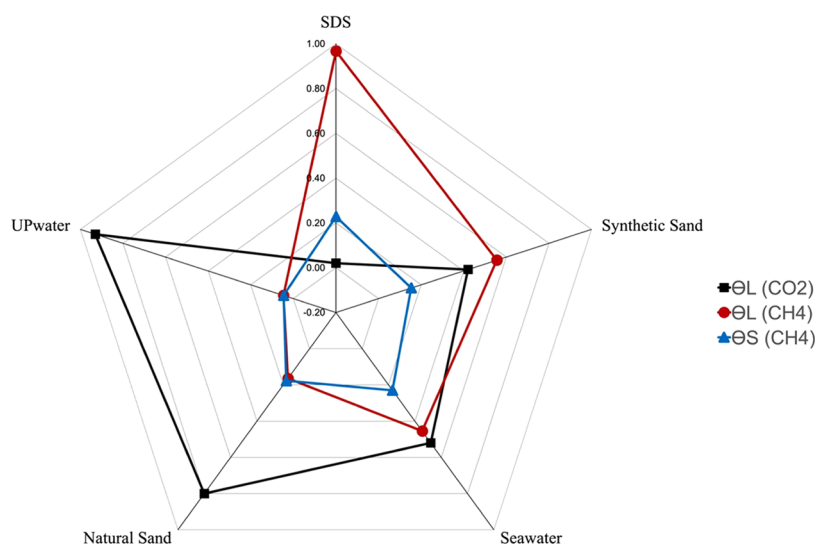
Figure 7. Plot showing the CH_4 and CO_2 occupancies in the small and large cages and the relative ratio.
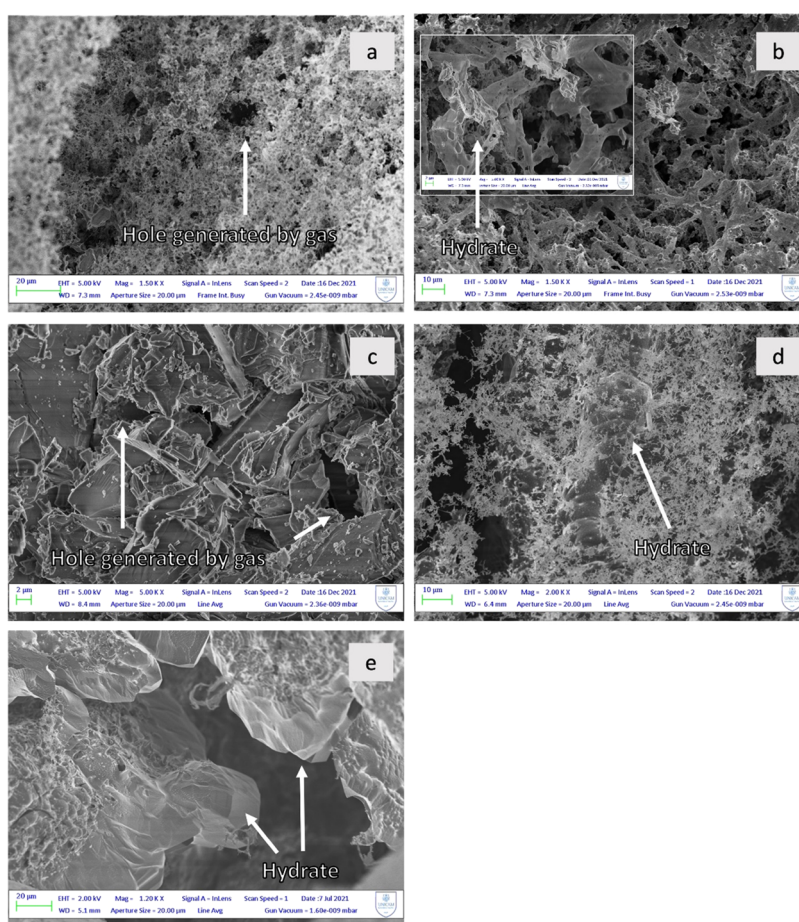

Figure 8. SEM images of CH_4-hydrates in (a) seawater, (b) SDS, (c) natural sand, (d) synthetic sand, and (e) UP water.

variations can affect the stability of CH_4-hydrates, and a constant pressure replacement process permits the reduction of these variations, preserving the hydrate structure during the gas exchange process. All Raman spectra, reported in Figure 6, were normalized to the isosbestic point of the OH band, as previously discussed. The cage occupancy, calculated by the vdWP thermodynamic model, showed a different trend with respect to that observed in the pure CH_4-hydrates.

Considering that CO_2 can preferentially occupy the large cavity,[11] and CH_4 can occupy both large and small cages, the thermodynamic expression from van der Waals and Platteeuw can be rearranged to calculate the occupancy of CO_2 in the large cavity and CH_4 in both cavities (eq 1)[9]
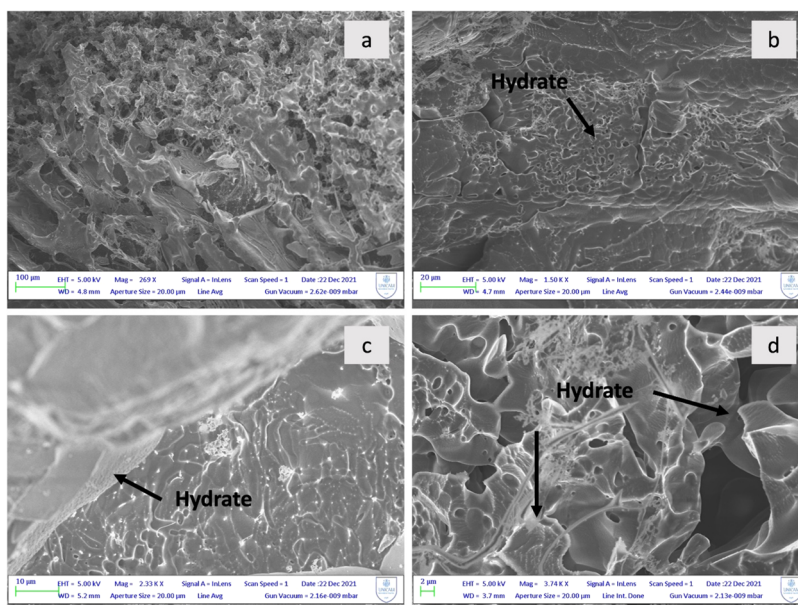
Figure 9. SEM images of CO_2-hydrates in (a) seawater, (b) SDS, (c) natural sand, and (d) synthetic sand.
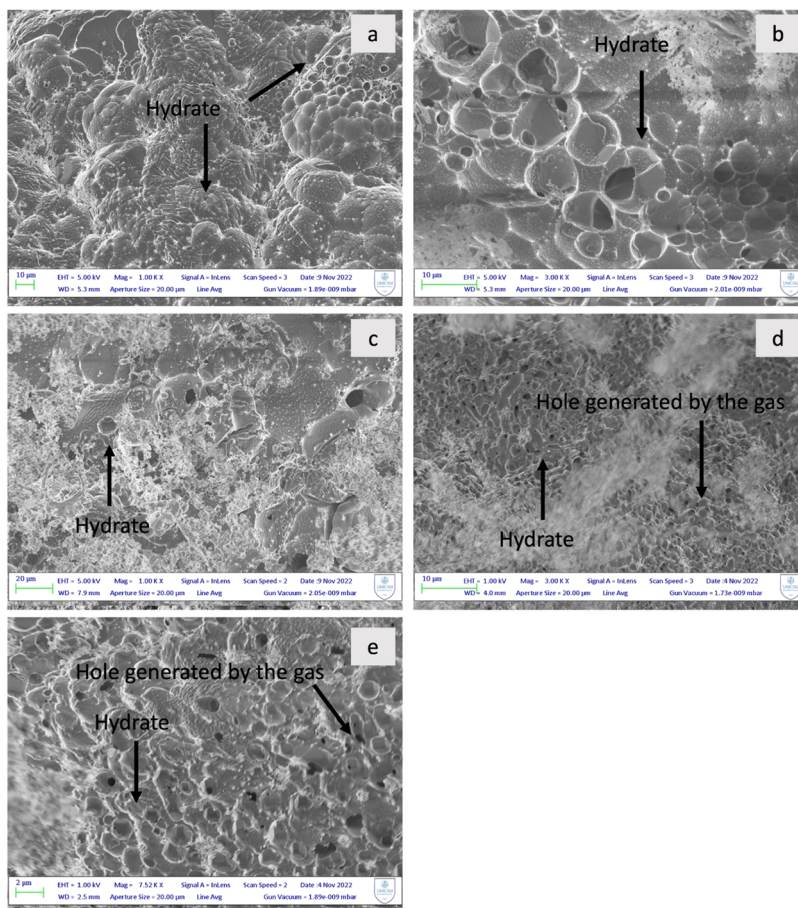

Figure 10. SEM images of CO_2/CH_4-hydrates in (a) SDS, (b) natural sand, (c) synthetic sand, (d) UP water, and (e) seawater.

$$\Delta\mu_w^H(T, P) = -RT[\nu_s \log(1 - \theta_{s,CH_4}) + \nu_1$$
$$\log(1 - \theta_{l,CO_2} - \theta_{l,CH_4})] \qquad (1)$$

where $\Delta\mu_w^H(T,P)$ is the chemical potential difference between the empty gas hydrate lattice and the stable ice lattice, and ν_1 and

ν_s represent the ratio of the large cage and small cage to the number of water molecules in the hydrate lattice, respectively. Since $CH_4 + CO_2$ also forms sI hydrates, the same value of $\Delta\mu_w(h°) = 1297$ J/mol, as for CH_4-hydrate, can be used as well as $\nu_s = 1/23$, $\nu_1 = 3/23$. As a result, the hydration number of CH_4/CO_2-hydrates can be calculated by eq 2

$$n = \frac{23}{(3\theta_{l,CH_4} + \theta_{s,CH_4} + 3\theta_{l,CO_2})} \quad (2)$$

The results of the cage occupancy calculation showed that the hydrate prepared in SDS showed the smallest degree of CH_4 replacement with CO_2; contrarily, the hydrate in UP water displayed the highest degree of replacement as predicted by the Gibbs free-energy calculation.[28] Interestingly, the hydrates in natural sand and, to a lesser extent, the hydrates in seawater (which are the most representative of the natural environment) showed a quite good degree of replacement (Figure 7). The striking differences in the θ_l values for the CO_2 and CH_4 in UP water vs SDS solution can be ascribed to the known CH_4 hydrate promotion effect of SDS over the CO_2 hydrates.[15] As a confirmation of this, θ_l for CO_2 in UP water is much larger than θ_l for methane, as would be clearly predictable from the much higher solubility of CO_2 in nonpromoted water.[15]

The observed differences between synthetic and natural sands are smaller and can be ascribed to the presence of metal oxides in the natural sand, in particular, ZnO, which is a known CO_2 promoter.[29]

The morphological characterization by SEM images shows clear evidence of hydrate structures in the CH_4-hydrates prepared in natural sand, synthetic sand, and UP water (Figure 8c,d,e) due to the presence of a dense and smooth surface, which is characteristic of a hydrate texture.[30] On the contrary, the SEM pictures of CH_4-hydrates, obtained in the presence of seawater and SDS, show a jagged surface; nevertheless, it was possible to ascertain the presence of a hydrated phase thanks to the presence of holes created by the release of gas upon beam irradiation (Figure 8a,b) as reported elsewhere.[31]

Figure 9 shows the SEM pictures of CO_2-hydrates prepared with seawater, where a jagged surface was observed, while the samples prepared in SDS, synthetic sand, and natural sand again show a smooth surface, which is characteristic of hydrate morphology.[30]

Finally, the morphological characterization of CO_2/CH_4-hydrate upon the exchange experiment (Figure 10) shows the typical morphology of hydrate in all of the investigated samples in addition to the presence of holes generated by the gas leaks under the effect of beam irradiation, indicating the presence of hydrates in all investigated samples.[30,31]

4. CONCLUSIONS

In this study, CO_2-, CH_4-, and CO_2/CH_4-hydrates were produced in different media, namely, SDS, natural sand, synthetic sand, UP water, and seawater and were successfully ex situ-characterized through Raman spectroscopy and scanning electron microscopy. The isobaric gas swapping proved to be an effective method for the preparation of the mixed hydrates, allowing it to decrease the chemical and physical disturbances to the system during the exchange process; notably, the constant pressure can also help to stabilize the temperature inside the reactor, preserving the hydrate structure during the gas exchange process. The morphological analysis of GHs by SEM analysis allowed us to highlight the peculiarity of the investigated hydrates, showing differences that are related to the media in which GHs were prepared. The GH characterization by ex situ Raman spectroscopy allowed us to calculate the cage occupancy and the hydration number of hydrates in several environmental conditions from the ratio of the areas corresponding to the small and large cavities. The Raman characterization of CH_4-hydrates indicated a high occupation of large cages in all samples (>96%)

and a high variability in the occupation of small cages; values of hydration numbers comparable to those reported in the literature were also found. The media effects in the exchange process were investigated by the calculation of the cage occupancies of the CO_2/CH_4-hydrates obtained after the replacement process, and from the results, pure water was identified as the best medium to conduct the exchange process. Interestingly, when natural sand and seawater were used to prepare the hydrates, a noticeable amount of CH_4 was displaced by CO_2. Lastly, the calculation and comparison of S_D indices allowed the estimation of the structural rigidity among the investigated samples. The data obtained in this study add more pieces to the literature information to develop an efficient CH_4/CO_2 replacement process.

■ ASSOCIATED CONTENT

Ⓢ Supporting Information

The Supporting Information is available free of charge at https://pubs.acs.org/doi/10.1021/acs.energyfuels.3c02991

Additional experimental details: standardized Raman spectra for the determination of the S_D index (Figures S1−S3 and Table S1); details of the VDW and Platteeuw thermodynamic model; pressure and temperature profiles of hydrate formation (Figures S5−S8); chemical and physical characterization of the media (Table S2 and Figure S9); and deconvolution of Raman spectra for CH_4 in large and small cages (Figures S10 and S11) (PDF)

■ AUTHOR INFORMATION

Corresponding Authors

Pietro Di Profio − University "G. d'Annunzio" of Chieti-Pescara, 66100 Chieti, Italy; ⓞ orcid.org/0000-0002-8038-7940; Email: pietro.diprofio@unich.it

Rita Giovannetti − School of Science and Technology, Chemistry Division, ChIP Research Center, University of Camerino, 62032 Camerino, Italy; ⓞ orcid.org/0000-0001-8099-6028; Email: rita.giovannetti@unicam.it

Authors

Andrea Rossi − School of Science and Technology, Chemistry Division, ChIP Research Center, University of Camerino, 62032 Camerino, Italy

Michele Ciulla − University "G. d'Annunzio" of Chieti-Pescara, 66100 Chieti, Italy

Valentino Canale − University "G. d'Annunzio" of Chieti-Pescara, 66100 Chieti, Italy

Marco Zannotti − School of Science and Technology, Chemistry Division, ChIP Research Center, University of Camerino, 62032 Camerino, Italy

Marco Minicucci − School of Science and Technology, Physics Division, University of Camerino, 62032 Camerino, Italy

Complete contact information is available at:
https://pubs.acs.org/10.1021/acs.energyfuels.3c02991

Author Contributions

The manuscript was written through contributions of all authors. All authors have given approval to the final version of the manuscript.

Notes

The authors declare no competing financial interest.

■ REFERENCES

(1) Dong, H.; Wang, J.; Xie, Z.; Wang, B.; Zhang, L.; Shi, Q. Potential Applications Based on the Formation and Dissociation of Gas Hydrates. *Renewable Sustainable Energy Rev.* 2021, *143*, No. 110928.

(2) Yang, L.; Liu, Y.; Zhang, H.; Xiao, B.; Guo, X.; Wei, R.; Xu, L.; Sun, L.; Yu, B.; Leng, S.; Li, Y. The Status of Exploitation Techniques of Natural Gas Hydrate. *Chin. J. Chem. Eng.* 2019, *27* (9), 2133−2147.

(3) Tamaki, M.; Fujimoto, A.; Boswell, R.; Collett, T. S. Geological Reservoir Characterization of a Gas Hydrate Prospect Associated with the Hydrate-01 Stratigraphic Test Well, Alaska North Slope. *Energy Fuels* 2022, *36* (15), 8128−8149.

(4) Liu, T.; Wu, P.; Chen, Z.; Li, Y. Review on Carbon Dioxide Replacement of Natural Gas Hydrate: Research Progress and Perspectives. *Energy Fuels* 2022, *36* (14), 7321−7336.

(5) Xu, C.-G.; Cai, J.; Yu, Y.-S.; Yan, K.-F.; Li, X.-S. Effect of Pressure on Methane Recovery from Natural Gas Hydrates by Methane-Carbon Dioxide Replacement. *Appl. Energy* 2018, *217*, 527−536.

(6) Wang, Y.; Lang, X.; Fan, S.; Wang, S.; Yu, C.; Li, G. Review on Enhanced Technology of Natural Gas Hydrate Recovery by Carbon Dioxide Replacement. *Energy Fuels* 2021, *35* (5), 3659−3674.

(7) Zhu, Y.-J.; Xie, Y.; Zhong, J.-R.; Wang, X.-H.; Xiao, P.; Sun, C.-Y.; Chen, G.-J. Mini Review on Application and Outlook of In Situ Raman Spectrometry in Gas Hydrate Research. *Energy Fuels* 2022, *36* (18), 10430−10443.

(8) Luzi, M.; Schicks, J. M.; Naumann, R.; Erzinger, J. Systematic Kinetic Studies on Mixed Gas Hydrates by Raman Spectroscopy and Powder X-Ray Diffraction. *J. Chem. Thermodyn.* 2012, *48*, 28−35.

(9) Sum, A. K.; Burruss, R. C.; Sloan, E. D. Measurement of Clathrate Hydrates via Raman Spectroscopy. *J. Phys. Chem. B* 1997, *101* (38), 7371−7377.

(10) Le, Q.-D.; Rodriguez, C. T.; Legoix, L. N.; Pirim, C.; Chazallon, B. Influence of the Initial CH4-Hydrate System Properties on CO2 Capture Kinetics. *Appl. Energy* 2020, *280*, No. 115843.

(11) Zhou, X.; Zang, X.; Long, Z.; Liang, D. Multiscale Analysis of the Hydrate Based Carbon Capture from Gas Mixtures Containing Carbon Dioxide. *Sci. Rep.* 2021, *11* (1), No. 9197.

(12) Platteeuw, J. C.; van der Waals, J. H. Thermodynamic Properties of Gas Hydrates. *Mol. Phys.* 1958, *1* (1), 91−96.

(13) Cha, M.; Shin, K.; Lee, H.; Moudrakovski, I. L.; Ripmeester, J. A.; Seo, Y. Kinetics of Methane Hydrate Replacement with Carbon Dioxide and Nitrogen Gas Mixture Using in Situ NMR Spectroscopy. *Environ. Sci. Technol.* 2015, *49* (3), 1964−1971.

(14) Canale, V.; Fontana, A.; Siani, G.; Di Profio, P. Hydrate Induction Time with Temperature Steps: A Novel Method for the Determination of Kinetic Parameters. *Energy Fuels* 2019, *33* (7), 6113−6118.

(15) Di Profio, P.; Canale, V.; D'Alessandro, N.; Germani, R.; Di Crescenzo, A.; Fontana, A. Separation of CO₂ and CH₄ from Biogas by Formation of Clathrate Hydrates: Importance of the Driving Force and Kinetic Promoters. *ACS Sustainable Chem. Eng.* 2017, *5* (2), 1990−1997.

(16) Di Profio, P.; Canale, V.; Germani, R.; Arca, S.; Fontana, A. Reverse Micelles Enhance the Formation of Clathrate Hydrates of Hydrogen. *J. Colloid Interface Sci.* 2018, *516*, 224−231.

(17) Wang, Z.; Pakoulev, A.; Pang, Y.; Dlott, D. D. Vibrational Substructure in the OH Stretching Transition of Water and HOD. *J. Phys. Chem. A* 2004, *108* (42), 9054−9063.

(18) Seki, T.; Chiang, K.-Y.; Yu, C.-C.; Yu, X.; Okuno, M.; Hunger, J.; Nagata, Y.; Bonn, M. The Bending Mode of Water: A Powerful Probe for Hydrogen Bond Structure of Aqueous Systems. *J. Phys. Chem. Lett.* 2020, *11* (19), 8459−8469.

(19) Walrafen, G. E. Raman and Infrared Spectral Investigations of Water Structure. In *The Physics and Physical Chemistry of Water*; Springer New York: Boston, MA, 1972; pp 151−214.

(20) Giovannetti, R.; Maria Gambelli, A.; Castellani, B.; Rossi, A.; Minicucci, M.; Zannotti, M.; Li, Y.; Rossi, F. May Sediments Affect the Inhibiting Properties of NaCl on CH4 and CO2 Hydrates Formation? An Experimental Report. *J. Mol. Liq.* 2022, *359*, No. 119300.

(21) Giovannetti, R.; Gambelli, A. M.; Rossi, A.; Castellani, B.; Minicucci, M.; Zannotti, M.; Nicolini, A.; Rossi, F. Thermodynamic Assessment and Microscale Raman Spectroscopy of Binary CO2/CH4 Hydrates Produced during Replacement Applications in Natural Reservoirs. *J. Mol. Liq.* 2022, *368*, No. 120739.

(22) Đuričković, I.; Marchetti, M.; Claverie, R.; Bourson, P.; Chassot, J.-M.; Fontana, M. D. Experimental Study of NaCl Aqueous Solutions by Raman Spectroscopy: Towards a New Optical Sensor. *Appl. Spectrosc.* 2010, *64* (8), 853−857.

(23) Frezzotti, M. L.; Tecce, F.; Casagli, A. Raman Spectroscopy for Fluid Inclusion Analysis. *J. Geochemical Explor.* 2012, *112*, 1−20.

(24) Kumar, R.; Englezos, P.; Moudrakovski, I.; Ripmeester, J. A. Structure and Composition of CO₂/H₂ and CO₂/H₂/C₃H₈ Hydrate in Relation to Simultaneous CO₂ Capture and H₂ Production. *AIChE J.* 2009, *55* (6), 1584−1594.

(25) Fleyfel, F.; Devlin, J. P. Carbon Dioxide Clathrate Hydrate Epitaxial Growth: Spectroscopic Evidence for Formation of the Simple Type-II Carbon Dioxide Hydrate. *J. Phys. Chem. A* 1991, *95* (9), 3811−3815.

(26) Subramanian, S.; Sloan, E. D. Trends in Vibrational Frequencies of Guests Trapped in Clathrate Hydrate Cages. *J. Phys. Chem. B* 2002, *106* (17), 4348−4355.

(27) Rauh, F.; Mizaikoff, B. Spectroscopic Methods in Gas Hydrate Research. *Anal. Bioanal. Chem.* 2012, *402* (1), 163−173.

(28) Yezdimer, E. M.; Cummings, P. T.; Chialvo, A. A. Determination of the Gibbs Free Energy of Gas Replacement in SI Clathrate Hydrates by Molecular Simulation. *J. Phys. Chem. A* 2002, *106* (34), 7982−7987.

(29) Mohammadi, M.; Haghtalab, A.; Fakhroueian, Z. Experimental Study and Thermodynamic Modeling of CO2 Gas Hydrate Formation in Presence of Zinc Oxide Nanoparticles. *J. Chem. Thermodyn.* 2016, *96*, 24−33.

(30) Sun, J.; Li, C.; Hao, X.; Liu, C.; Chen, Q.; Wang, D. Study of the Surface Morphology of Gas Hydrate. *J. Ocean Univ. China* 2020, *19* (2), 331−338.

(31) *Water-Rock Interaction, Two Vol. Set*; Wanty, R. B.; Seal, R. R., II, Eds.; CRC Press, 2004.